

Article

A Polydnavirus Protein Tyrosine Phosphatase Negatively Regulates the Host Phenoloxidase Pathway

Hong-Shuai Gao^{1,2,3,4} , Rong-Min Hu^{1,3,4}, Ze-Hua Wang^{1,3,4}, Xi-Qian Ye^{1,2,3,4}, Xiao-Tong Wu^{1,3,4}, Jian-Hua Huang^{1,2,3,4} , Zhi-Zhi Wang^{1,2,3,4,5,*}  and Xue-Xin Chen^{1,2,3,4}

¹ Institute of Insect Sciences, College of Agriculture and Biotechnology, Zhejiang University, Hangzhou 310058, China

² Guangdong Laboratory for Lingnan Modern Agriculture, Guangzhou 510642, China

³ Ministry of Agriculture Key Laboratory of Molecular Biology of Crop Pathogens and Insects, Zhejiang University, Hangzhou 310058, China

⁴ Key Laboratory of Biology of Crop Pathogens and Insects of Zhejiang Province, Zhejiang University, Hangzhou 310058, China

⁵ The Rural Development Academy, Zhejiang University, Hangzhou 310058, China

* Correspondence: zzwang0730@zju.edu.cn

Abstract: Polydnavirus (PDV) is a parasitic factor of endoparasitic wasps and contributes greatly to overcoming the immune response of parasitized hosts. Protein tyrosine phosphatases (PTPs) regulate a wide variety of biological processes at the post-transcriptional level in mammals, but knowledge of PDV PTP action during a parasitoid–host interaction is limited. In this study, we characterized a PTP gene, *CvBV_12-6*, derived from *Cotesia vestalis* bracovirus (CvBV), and explored its possible regulatory role in the immune response of the host *Plutella xylostella*. Our results from qPCR show that *CvBV_12-6* was highly expressed in hemocytes at an early stage of parasitization. To explore *CvBV_12-6* function, we specifically expressed *CvBV_12-6* in *Drosophila melanogaster* hemocytes. The results show that Hml-Gal4 > *CvBV_12-6* suppressed the phenoloxidase activity of hemolymph in *D. melanogaster*, but exerted no effect on the total count or the viability of the hemocytes. In addition, the Hml-Gal4 > *CvBV_12-6* flies exhibited decreased antibacterial abilities against *Staphylococcus aureus*. Similarly, we found that *CvBV_12-6* significantly suppressed the melanization of the host *P. xylostella* 24 h post parasitization and reduced the viability, but not the number, of hemocytes. In conclusion, *CvBV_12-6* negatively regulated both cellular and humoral immunity in *P. xylostella*, and the related molecular mechanism may be universal to insects.

Keywords: protein tyrosine phosphatase; polydnavirus; phenoloxidase



Citation: Gao, H.-S.; Hu, R.-M.; Wang, Z.-H.; Ye, X.-Q.; Wu, X.-T.; Huang, J.-H.; Wang, Z.-Z.; Chen, X.-X. A Polydnavirus Protein Tyrosine Phosphatase Negatively Regulates the Host Phenoloxidase Pathway. *Viruses* **2023**, *15*, 56. <https://doi.org/10.3390/v15010056>

Academic Editor: A. Lorena Passarelli

Received: 18 November 2022
Revised: 19 December 2022
Accepted: 21 December 2022
Published: 24 December 2022



Copyright: © 2022 by the authors. Licensee MDPI, Basel, Switzerland. This article is an open access article distributed under the terms and conditions of the Creative Commons Attribution (CC BY) license (<https://creativecommons.org/licenses/by/4.0/>).

1. Introduction

Polydnaviruses (PDVs) are large double-stranded circular DNA (dsDNA) viruses that can be classified into bracoviruses (BVs) and ichnoviruses (IVs) according to their mutualistic relationship with braconid and ichneumonid wasps [1,2]. PDVs persist in a given wasp genome as proviruses with two distinct parts: structural core genes that are critical for the formation of virion particles, and proviral segments that serve as templates for the production of the virulence genes in its secondary host, primarily an insect in the Lepidoptera order [3]. These virulence genes alter host physiology, growth, and development, facilitating the survival of wasp offspring [1,4–7]. They are classified into gene families and contribute greatly to host immunosuppression and growth regulation [6,8,9]. Several BV virulence genes have been demonstrated to disrupt multiple elements of a host's immune system. For example, two genes in *Microplitis demolitor* BV (MdBV), Egf 1.0 and Egf 1.5, which carry an epidermal growth-factor-like motif, have been demonstrated to inhibit melanization by targeting phenoloxidase-activating proteinase (PAP) [10,11]. Two members of the BV ankyrin gene family function as mimics of IκB proteins, and target the

host nuclear factor- κ B pathway to suppress the expression of antimicrobial peptides [12,13]. Recently, *Microplitis bicoloratus* bracovirus was found to induce apoptosis in host hemocytes by activating caspase-3 and suppressing the immune response by reducing the phosphorylation level of components of the p13K/AKT signaling pathway [14,15]. Notably, the function of many other PDV genes is unknown.

In vertebrates, protein tyrosine phosphatases (PTPs), which catalyze the removal of the phosphate group from a tyrosine residue in a target protein, are indispensable and specific modulators of cellular signaling, thus regulating many processes, such as cell convergence and extension [16], cell differentiation [17–20], the signal transduction pathways in immunity [21–23], and metabolism-related pathways [24]. The structurally conserved PTP domain is key to membership in the PTP family, and three PTP groups have been categorized to date: (i) classical PTPs, (ii) PTPs with dual-specificity, and (iii) low-molecular-weight PTPs [25]. The PTP gene family has been found in the most extensively sequenced BV genome and constitutes the largest PDV gene family, except for the recently sequenced CinsBV of the *Chelonius insularis* wasp that does not contain PTP genes [26–34]. The BV PTP gene family expanded via classical mechanisms, including segmental duplication, tandem duplication, and dispersed duplication [35]. Bracovirus PTPs belong to the classical PTP family, and are characterized by their highly comparable PTP domain to vertebrate PTPs, with some carrying other functional domains [36]. Despite their sequence similarity, in contrast to classical PTPs, it is unclear whether the bracovirus PTPs are functional because they are highly divergent and lack conserved domains for substrate specificity, as proven by the fact that some BV PTPs are functional tyrosine phosphatases, whereas others are not [37,38]. Several BV PTPs have been demonstrated to suppress host immunity. For example, PTP-H2 and PTP-H3 of MdBV showed tyrosine phosphatase activity and involvement in the inhibition of phagocytosis by S2 cells [38]; Richard et al. [39] confirmed that the phosphatase activity of PTP-H2 in MdBV is critical for the induction of cell apoptosis. Hemocytes expressing PTP1 derived from *Cotesia vestalis* bracovirus (CvBV) exhibit a significant reduction in both cell spreading and encapsulation [40]. In addition, recent research has shown that a PTP from *Toxoneuron nigriceps* BV participates in the blockade of ecdysteroidogenesis, possibly by disrupting the phosphorylation balance of key proteins in the MAPK and PI3K ecdysone pathways, altering host growth and development [41,42]. However, the role of most BV PTPs in host–parasitoid interactions has not been well elucidated.

Cotesia vestalis (Haliday) is a major natural enemy of *Plutella xylostella* (L.) (Lepidoptera: Plutellidae), a destructive pest of Brassica crops worldwide [43]. Our previous studies showed that the CvBV genome is composed of 30 DNA segments that encode 218 genes in 13 gene families, with CvBV-PTP constituting the largest gene family (with 33 PTP genes) [44]. In this study, we focused on characterizing the immunosuppressive role of CvBV-PTP genes. We found a PTP gene, designated CvBV_12-6, encoded by the 6th gene in the 12th segment of the CvBV genome. CvBV_12-6 was verified to show phosphatase activity. Ectopic expression of CvBV_12-6 in the *D. melanogaster* model suppressed the phenoloxidase (PO) activity of hemolymph and increased the susceptibility to *Staphylococcus aureus*. Furthermore, we found that CvBV_12-6 inhibited cellular immunity and humoral immunity in the *P. xylostella* host by reducing the hemocyte viability and suppressing the PO activity in the host hemolymph.

2. Materials and Methods

2.1. Insect Rearing

Plutella xylostella and its endoparasitoid *Cotesia vestalis* were reared as previously described [45]. They were maintained in a 14 h light/10 h dark photoperiod at 25 ± 1 °C with 65% relative humidity. Adult *P. xylostella* and *C. vestalis* were fed a 20% honey/water (V/V) solution. To ensure a high parasitization rate, middle third instar host individuals were exposed to a single female wasp within a test tube until oviposition was observed. W1118 wild-type and Bloomington Hml-GAL4 (BDSC_30140) *D. melanogaster* stock was

used in this study, and the flies were reared on standard cornmeal/yeast/agar medium at 18 °C.

2.2. Sequence Analysis

According to the annotated CvBV genome, the sequences of CvBV_12-6 were downloaded. The signal sequence was predicted by SignalP 6.0 (<https://services.healthtech.dtu.dk/service.php?SignalP>, accessed on 2 January 2021). Multiple sequence alignment was performed with DNAMAN (V10.0.2.128) software.

2.3. RNA Extraction and ORF Cloning

RNA was extracted from five *P. xylostella* larvae at 12 h, 24 h, 48 h, and 96 h post parasitization (pp), respectively. TRIzol reagent (Invitrogen, Carlsbad, CA, USA) was used to isolate total RNA according to the manufacturer's instructions. RNA purity was determined with a NanoDrop[®] spectrophotometer (Thermo Fisher, Waltham, MA, USA). A SuperScript[™] III Reverse Transcriptase kit (Vazyme, Nanjing, China) was used to synthesize a complementary DNA (cDNA) library. The primers used for PCR are shown in Table 1. PCR was performed under the following cycling conditions: 94 °C for 2 min, 35 cycles of 95 °C for 30 s, 60 °C (according to different primers inducing change) for 30 s, and 72 °C for 15 s, and then 72 °C for 10 min. Each PCR product was cleaned with a Wizard[®] SV Gel and PCR Clean-Up System (Promega, Madison, WI, USA) kit, and then cloned into a pGEM-T Easy Vector. Recombinant vectors were transferred into the *E. coli* TG1 strain, and positive clones were sequenced by Sangon (Shanghai, China). The sequenced fragments were assembled by SeqMan software (DNASTAR, 7.1.0.44 version), and then aligned with the CvBV genome with BLASTP (<http://www.ncbi.nlm.nih.gov/>, accessed on 2 February 2021).

Table 1. The primer sequences for functional studies of CvBV-PTP24.

Primer Name	Primer Sequence (5' to 3')	Purpose
PTP24-orf-SP	AAATGAGTTCTAACAAAGGCG	gene cloning
PTP24-orf-AP	TGTTGTCCCAGACCATTITTC	gene cloning
PTP24-qrt-SP	TCGACAGCTTCAAACAACCC	qPCR
PTP24-qrt-AP	GTCGCCCCGTTCTTCCAATT	qPCR
Px- β -tubulin-SP	GACGCATGTCCATGAAGGAG	qPCR
Px- β -tubulin-AP	CCAATGCAAGAAAGCCTTGC	qPCR
PTP24-BamHI-SP	CGCGGATCCATGAGTTCTAACAAAG	eukaryotic expression
PTP24-XhoI-AP	CCGCTCGAGTTACGTATAAAGATT	eukaryotic expression and transgenic fruit fly
PTP24-NotI-SP	ATTTGCGGCCGCATGAGTTCTAACAAAG	transgenic fruit fly
PTP24-dsRNA-SP	GGTCTGGGAACAACAATCTG	RNAi
PTP24-dsRNA-AP	TCTCAGTTGGGACACGATAG	RNAi
PTP24-dsRNA-SP-T7	TAATACGACTCACTATAGGGGTCTGGGAACAACAATCTG	RNAi
PTP24-dsRNA-AP-T7	TAATACGACTCACTATAGGTCTCAGTTGGGACACGATAG	RNAi
GFP-dsRNA-SP	CAGTGCTTCAGCCGCTACCC	RNAi
GFP-dsRNA-AP	CTTCTCGTTGGGGTCTTTGCT	RNAi
GFP-dsRNA-SP-T7	TAATACGACTCACTATAGGCAGTTCAGCCGCTACCC	RNAi
GFP-dsRNA-AP-T7	TAATACGACTCACTATAGGCTTCTCGTTGGGGTCTTTGCT	RNAi

2.4. Expression Analyses by qPCR

To analyze gene expression levels in different developmental stages, five *P. xylostella* larvae were collected as RNA samples 6 h, 12 h, 24 h, 48 h, 72 h, 96 h, and 120 h after parasite exposure. qPCR was performed as previously described [46]. A ReverTra Ace qPCR RT kit (Toyobo, Osaka, Japan) was used to synthesize cDNAs. The primers used for qPCR are shown in Table 1. β -Tubulin (GenBank accession No. EU127912) from *P. xylostella* was used as the reference gene. qPCRs were performed on a CFX Connect real-time system (Bio-Rad, Hercules, CA, USA) using THUNDERBIRD qPCR Mix (Toyobo, Osaka, Japan). Each qPCR for a given gene and time point was performed using at least three biological replicates under the following cycling conditions: 95 °C for 60 s, 40 cycles of 95 °C for 15 s, and 60 °C for 30 s. The results were analyzed via the $2^{-\Delta\Delta CT}$ method.

Similarly, to detect the tissue preference of *CvBV_12-6* in a host, hemocytes and tissues, i.e., central nervous system (CNS), fat body, midgut, cuticle, testis, silk gland, and malpighian tubule tissues, from different developmental stages of parasitized larvae (30 larvae per sample) were dissected in phosphate-buffered saline (PBS) and then subjected to qPCR. The qPCR program was the same as that described above. All assays were performed at least three times.

2.5. Recombinant Baculovirus Concentration

The pFASTBAC-HTb (Invitrogen, San Diego, CA, USA) vector for baculovirus expression in *P. xylostella* hemocytes was modified by inserting the open reading frame (ORF) sequence of *CvBV_12-6* with an HA tag using conventional molecular biology techniques. The GFP gene was used as the negative control, and the sequence was cloned from a pRSET-eGFP vector (Thermo, USA, V35320). The primers used are shown in Table 1. Recombinant nucleopolyhedroviruses (NPVs), NPV-*CvBV_12-6* or NPV-*GFP*, were produced with a Bac-to-Bac Baculovirus Expression System (Invitrogen, San Diego, CA, USA) according to the manufacturer's instructions. The recombinant NPVs were concentrated by centrifugation as described by [47] and then resuspended in 100 μ L of PBS buffer (pH 7.4). The titer of the generated high-titer virus stock was determined by viral plaque assay according to the Bac-to-Bac Baculovirus Expression System manufacturer instructions (Invitrogen, San Diego, CA, USA). An overexpression experiment was performed by injecting 1×10^5 copies of NPV-*CvBV_12-6* or NPV-*GFP* into third instar *P. xylostella* larvae.

2.6. Tyrosine Phosphatase Assay and Western Blotting

For convenient protein collection, the recombinant baculovirus NPV-*CvBV_12-6* and NPV-*GFP* (5×10^7 copies) were expressed in Sf9 cells (5×10^6 cells), which were cultured at 27 °C in a cell incubator. All the cells were collected 2 days later and washed with PBS at least three times. The clean cells were lysed with a reagent (Promega, Madison, WI, USA), and the following procedure was performed according to the instructions of a tyrosine phosphatase assay kit (Promega, Madison, WI, USA). The activity of tyrosine phosphatase depends on the concentration of free phosphate, which can be reflected by the absorbance read at 630 nm.

The recombinant *CvBV_12-6* protein from Sf9 cells was detected by western blot using an HA monoclonal antibody (Sangon, Shanghai, China), and an anti-Actin monoclonal antibody (Sangon, Shanghai, China) was used as the internal control. Samples were diluted in 5 \times protein sodium dodecyl sulfate–polyacrylamide gel electrophoresis loading buffer (Sangon, Shanghai, China) and then boiled for 10 min. The proteins in the samples separated in the denaturing polyacrylamide gel were transferred to a polyvinylidene difluoride membrane. After blocking and washing, the membranes were incubated with primary antibodies against HA or actin (1: 10,000) for 2 h at room temperature. The membranes were then incubated with horseradish peroxidase-conjugated goat anti-mouse IgG secondary antibody diluted 1:3000 in Tris-buffered saline with Tween-20. After washing five times, the membranes were incubated with enhanced chemiluminescence western blot substrate (Promega, Madison, WI, USA).

2.7. Transgenic Fly Construction

The GAL4/UAS (upstream activator sequence) binary expression system was used to study the function of *CvBV_12-6* in *D. melanogaster* [48]. The open reading frame (ORF) sequence of *CvBV_12-6* was cloned into a pUAST-attb vector [49]. A transgenic fly carrying the UAS-*CvBV_12-6* gene was obtained by phiC31 integrase-mediated insertion into the attP2 landing site locus on the third chromosome. We used Hml-GAL4 (BDSC_30140), an expression driver of lymph glands and circulating hemocytes, to drive *CvBV_12-6* expression in the *D. melanogaster* hemocytes [50]. Thirty adult Hml-GAL4 strain males and 200 adult UAS-*CvBV_12-6* strain virgins were selected, mated for 1 day, and transferred to

a new food bottle every 2 h. Larvae from crosses of Hml-GAL4 and W1118 were used as controls.

2.8. RNA Interference

Double-stranded RNA (dsRNA) specific for *CvBV_12-6* and *GFP* was produced and purified using a T7 RiboMAXTM Express kit (Promega, Madison, WI, USA). The primers used for dsRNA synthesis are shown in Table 1. The synthesis products were confirmed by running dsRNA on an agarose gel; before parasitization, 1 µg of *CvBV_12-6* or *GFP* dsRNA was injected into third instar *P. xylostella* larvae using an Eppendorf Femto jet device (Eppendorf, Germany). The efficiency of the interference was determined individually by qPCR 12 h, 24 h, 36 h, and 48 h pp.

2.9. Hemocyte Count

The hemolymph of *P. xylostella* was collected 24 h after RNAi or injection of NPVs. A trypan blue stock solution was diluted to generate a 1× work solution, and 19.5 µL of the trypan blue work solution was mixed with 0.5 µL of hemolymph. This reagent was then added to a cell counting plate, and Countstar 1.0 software was used to determine the cell number and viability automatically using 6–15 µm as the initial detection parameter.

2.10. PO Activity Assays

PO activity was measured as previously described [51] with a minor modification to the procedure described by Goldsworthy et al. [52]. Approximately 5 µL of hemolymph from approximately 30 *P. xylostella* larvae 24 h post treatment was added to 95 µL of anticoagulant buffer (100 mmol/L glucose; 62 mmol/L NaCl; 30 mmol/L trisodium citrate; 26 mmol/L citric acid, and 10 mmol/L ethylenediaminetetraacetic acid, pH 4.6). To remove the hemocytes, the diluted hemolymph was centrifuged at 1000× *g* for 5 min. A Better Bradford AssayTM kit (Thermo, USA) was used to determine the protein concentration of each diluted cell-free hemolymph sample. Subsequently, 20 µL of heat-killed *Micrococcus luteus* (optical density (OD) = 0.5) was added to the diluted hemolymph and incubated for 20 min at room temperature. The mixture was then used to immediately measure the PO activity. PO activity was measured spectrophotometrically by recording the formation of dopachrome from L-dihydroxyphenylalanine (L-DOPA). Each assay was established in a 96-well plate with a total volume of 200 µL (with 140 µL of L-DOPA [3 g/L] and 60 µL of diluted cell-free hemolymph). The absorbance at 490 nm was measured once every 5 min for a total of 60 min. PO activity is expressed as a change in absorbance at 490 nm per mg protein per min. Each assay was performed with at least three biological replicates.

As for *D. melanogaster*, 30 adult Hml-GAL4 strain males and 200 adult UAS-*CvBV_12-6* or W1118 strain virgins were crossed and laid eggs in different bottles. The offspring in one bottle were used as a replicate. The hemolymph was collected from approximately 30 third instar offspring larvae and PO activity was measured as described above. The assay was replicated three times.

2.11. Survival Assay

A survival assay was performed as previously described [53]. *Staphylococcus aureus* is a gram-positive bacteria that is among the most frequent cause of morbidity and mortality due to infection worldwide [54]. The strength of the immune response of *D. melanogaster* larvae was measured to determine the risk of *S. aureus* infection. *S. aureus* was grown overnight at 37 °C with shaking at 250 r/min. Cultures were centrifuged at 1000× *g* for 1 min. The bacteria were resuspended in sterile PBS until an OD₆₀₀ of 0.4 was obtained. Seven days post eclosion, a male fly was injected with 40 nL of bacterial resuspension using an Eppendorf Femto jet device (Eppendorf, Germany) with a microcontroller (Narishige, Japan). Experiments were performed in triplicate (n = 20 flies per treatment). Injections were performed under a Stemi 2000-C microscope (Zeiss, Germany). Flies were reared at 25 °C after injection. Flies that died within 6 h were considered dead and removed from

in different tissues via qPCR. Our analysis shows that the transcriptional level of *CvBV_12-6* peaked 12 h post parasitization (pp) and then dropped gradually 24 h pp (Figure 1B). The expression of *CvBV_12-6* in different tissues showed that *CvBV_12-6* was expressed in all the tested tissues, with the highest transcript abundance in hemocytes and the second highest in the fat body. The expression level in the hemocytes at 12 h pp was at least 40-fold higher than that in the fat body, but its transcriptional level in the other six tissues was relatively low at each sampling time point (Figure 1C).

3.3. The *CvBV_12-6* Protein Exhibited Tyrosine Phosphatase Activity

To determine whether *CvBV_12-6* was functional, we collected Sf9 cells infected with the recombinant NPV-*CvBV_12-6* for 2 days and then extracted the total proteins. Compared with the uninfected Sf9 cells, western blot results show a clear band with a corresponding protein size of 40 kDa, which was slightly larger than the predicted size of *CvBV_12-6* (34.12 kDa) (Figure 2A). Compared with the NPV-*GFP* group, the cells that expressed *CvBV_12-6* released more free phosphate, indicating that *CvBV_12-6* showed tyrosine phosphatase activity (Figure 2B).

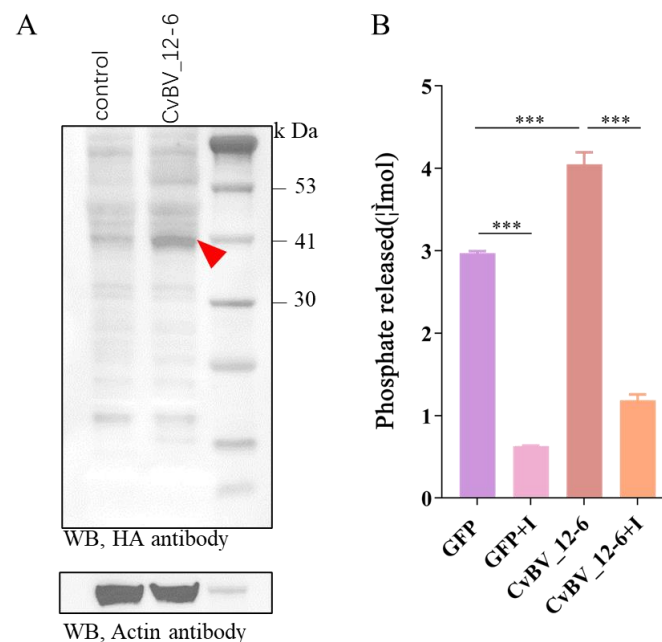


Figure 2. Eukaryotic expression of *CvBV_12-6* and tyrosine phosphatase activity detection. (A) The expression of *CvBV_12-6* in the Sf9 cell line was detected by western blotting using an HA tag monoclonal antibody, and actin was used as the internal control. (B) The tyrosine phosphatase activity of *CvBV_12-6* in Sf9 cells was measured by the amount of phosphate released after the incubation of the total protein and synthesized phosphopeptides. The cell lysate was extracted 48 h post infection. The GFP was used as the negative control, and sodium vanadate was used as the protein tyrosine phosphatase inhibitor (I). Data are presented as the mean \pm SD. Differences among samples were evaluated for significance via Tukey's test (***, significant difference at a p value < 0.001).

3.4. *CvBV_12-6* Negatively Regulates the Phenoloxidase Pathway in *D. melanogaster*

In contrast with those in Hml-Gal4 > W1118 flies, the total count and viability of hemocytes in third instar Hml-Gal4 > *CvBV_12-6* *D. melanogaster* larvae were not affected (Figure 3A,B). We measured the PO activity of hemolymph in the *D. melanogaster* larvae. The PO activity of hemolymph in Hml-Gal4 > *CvBV_12-6* larvae was significantly lower compared with that in Hml-Gal4 > W1118 flies (Figure 3C), suggesting a suppressive role for *CvBV_12-6* during melanization. In addition, Hml-Gal4 > *CvBV_12-6* flies showed increased susceptibility against *S. aureus* infection (Figure 3D), suggesting a decrease in antibacterial ability due to the expression of *CvBV_12-6*.

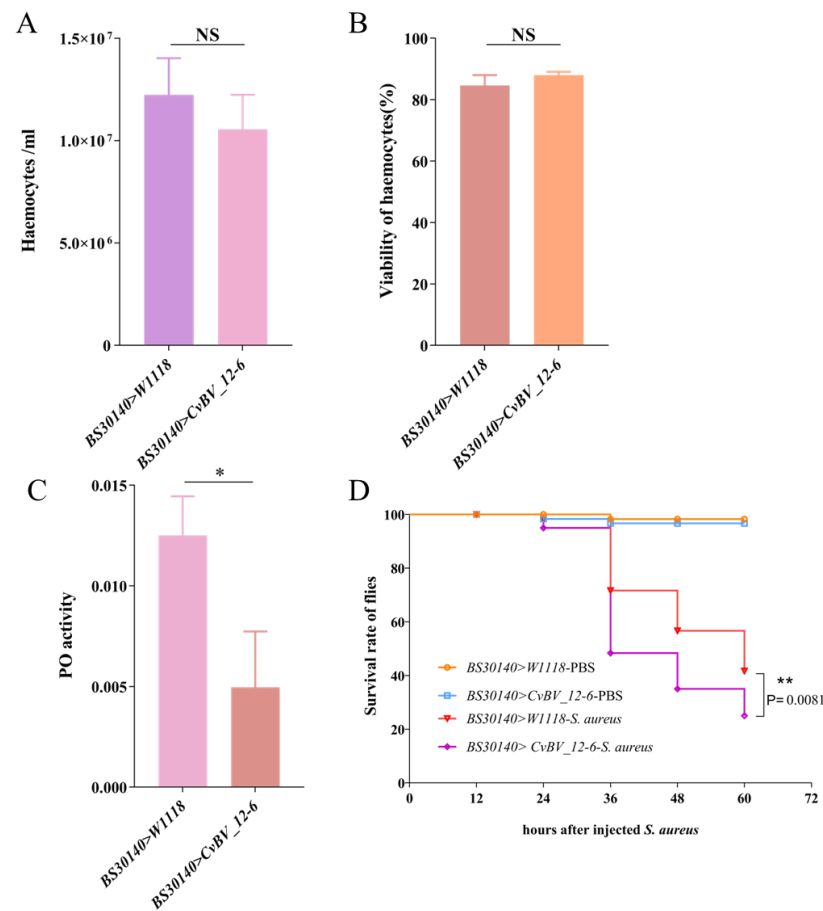


Figure 3. The immunosuppression of *CvBV_12-6* in *D. melanogaster*. **(A,B)** The effect of *CvBV_12-6* on the number **(A)** and the viability of hemocytes **(B)** in *D. melanogaster*. **(C)** The effect of *CvBV_12-6* on the PO activity in *D. melanogaster*. The hemolymph was collected from third instar *D. melanogaster* larvae, and the PO activity was determined as a change in absorbance at 490 nm per mg protein per min. **(D)** The antibacterial activity of male *D. melanogaster* to *S. aureus*. Thirty adult Hml-GAL4 strain males and 200 adult UAS-*CvBV_12-6* strain virgins were mated for 1 day and then transferred to a new food bottle every 2 h. Hml-GAL4 flies crossed with W1118 flies were the controls. Data are presented as the mean \pm SD from three independent experiments. Each treatment group included 20 larvae ($n = 15$). Differences among samples were evaluated for significance via Tukey's test (NS, no significance; *, significant difference at a p value < 0.05 ; **, significant difference at a p value < 0.01).

3.5. *CvBV_12-6* Decreases the Viability of Hemocytes in the *P. xylostella* Host

Considering the results with flies, we explored the immunosuppressive role played by *CvBV_12-6* in its natural host, *P. xylostella*. The expression level of *CvBV_12-6* was reduced by the injection of gene-specific dsRNA. Our results show that the relative expression level of *CvBV_12-6* was decreased by at least 40% 48 h after dsRNA injection (Figure 4A,B). Moreover, we overexpressed *CvBV_12-6* in *P. xylostella* by injecting recombinant NPV-*CvBV_12-6*. The injection dosage was calculated based on the standard curve (Figure 4C,D). Then, we injected 1×10^5 copies of recombinant baculoviruses according to the protocol of a Bac-to-Bac system; however, this concentration was not sufficient for infecting insect cells.

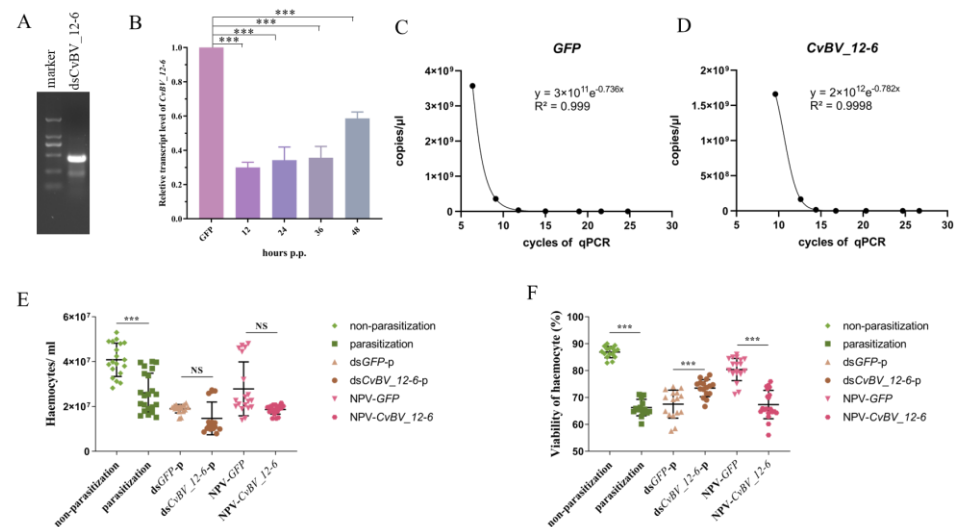


Figure 4. The effect of *CvBV_12-6* on hemocytes of the *P. xylostella* host. (A) The biosynthesis of dsRNA of *CvBV_12-6* was detected by agarose gel electrophoresis. (B) The RNA interference efficiency was measured by qPCR. (C,D) A standard curve was used to calculate the titer of the recombinant baculovirus as determined by qPCR. (E,F) The effect of *CvBV_12-6* on the hemocyte count and the hemocyte viability in *P. xylostella*. The hemolymph of *P. xylostella* was collected 24 h after parasitization, RNAi or injection of NPV. Then, 19.5 μ L of trypan blue working solution was mixed with 0.5 μ L hemolymph, and then added to a cell counting plate. Count Star 1.0 software was used to automatically analyze the cell number and viability. ds*CvBV_12-6*-p: ds*CvBV_12-6* was injected into third instar larvae, and parasitization was performed immediately; dsGFP-p was used as the negative control. NPV-*CvBV_12-6*: injection of NPV-*CvBV_12-6* into third instar larva; NPV-GFP was used as the negative control. Each treatment group included more than 30 larvae ($n > 15$). Data are presented as the mean \pm SD. Differences among samples were evaluated for significance via Tukey's test (***, significant difference for a p value < 0.001).

Compared with those of normal *P. xylostella* larvae, the total count and the viability of hemocytes were significantly decreased in parasitized hosts (Figure 4E,F). In addition, *CvBV_12-6* played a negative role in the viability of hemocytes, but exerted no effect on the total hemocyte count. Compared to the control group, the knockdown of *CvBV_12-6* significantly increased the viability of *P. xylostella* hemocytes, while the overexpression of *CvBV_12-6* by recombinant baculovirus injection significantly decreased the viability compared with that of the control baculovirus injection (Figure 4F).

3.6. *CvBV_12-6* Inhibits Melanization of *P. xylostella*

In *D. melanogaster*, we found that *CvBV_12-6* effectively suppresses the PO pathway; therefore, we hypothesized that its function in *P. xylostella* is the same. Considering the higher expression level of *CvBV_12-6* 12 h and 24 h pp and the parasitization by *C. vestalis* significantly suppressing PO activity of the host hemolymph 24 pp in previous research [55], we measured the PO activity of *P. xylostella* hemolymph 24 pp. As shown in Figure 5A, the PO activity was significantly increased at 24 h pp in the host larvae treated with ds*CvBV_12-6*. Consistent with that in parasitized hosts, the PO activity in the host hemolymph was significantly suppressed 24 h after *CvBV_12-6* was initially overexpressed (Figure 5B).

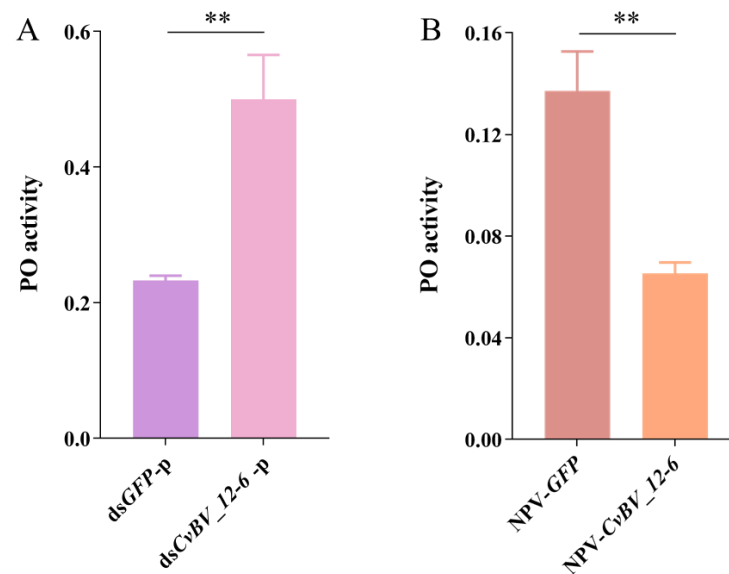


Figure 5. *CvBV_12-6* inhibited the melanization response of the *P. xylostella* host. (A) One microgram of ds*CvBV_12-6* or dsGFP was injected into third instar *P. xylostella* larvae, and parasitization was performed immediately. The hemolymph was collected, and the PO activity was measured 24 h pp. (B) NPV-*CvBV_12-6* or NPV-GFP was injected into third instar *P. xylostella* larvae, and the PO activity was measured 24 h post injection. Data are presented as the mean \pm SD. Differences among samples were evaluated for significance via Tukey's test (**, significant difference at a p value < 0.01).

4. Discussion

Polydnavirus-mediated disruption of cellular and humoral immunity renders parasitized lepidopteran larvae suitable for the development of wasp larvae as well as makes them susceptible to opportunistic infections [8]. In the *P. xylostella*–*C. vestalis* system, a series of PDV genes are delivered into the host genome to inhibit the host immune response and contribute greatly to successful parasitization [6,8,9]. In this study, we characterized a PTP gene, *CvBV_12-6*, encoded by *CvBV*, and explored its role in the immune response of the host.

Previous research had identified 10 conserved motifs in 113 vertebrate PTP domains, and these structural motifs were shown to work together to regulate the dephosphorylation process precisely [36]. The proposed role of each motif during dephosphorylation has been well characterized: Motifs 2 to 7 play key roles in stabilizing the secondary structure of the PTP domain; Motifs 1 and 8 are required for substrate recognition; Motifs 9 and 10 participate in substrate binding, catalysis, and optimal hydrolysis, respectively [36,37]. In our research, multiple sequence alignment showed that *CvBV_12-6* carries ten motifs, with most diverging from the motifs of classical vertebrate PTPs, except for Motif 2 and Motif 3 (Figure 1A). We speculate that this divergence probably evolved in the context of parasitism, which allowed parasites to recognize different substrates or similar substrates in different host species. In addition to this study, other BV PTPs, in which the motifs diverge from the classical motifs, have been demonstrated to exhibit tyrosine phosphatase activity; these PTPs include PTP-H2 and PTP-H3 from MdBV [38]. Notably, while four residues (D9, N12, S14, and I15) in Motif 9 of *CvBV_12-6* differ from those at these sites in classical PTPs, conservation of the cysteine (C6) site suggests that the PTP functions as a phosphatase, as described in previous papers [37,56,57]. This evidence suggests that whether bracovirus PTPs exhibit phosphatase activity does not entirely depend on the conservation of the motifs, but on the conservation of some important amino acid residues.

The expression of *CvBV_12-6* in different tissues reveals that *CvBV_12-6* was expressed in all the tested tissues with the highest transcript abundance in the hemocytes, which are critical for many immune responses in insects [58]. Hence, we infer that enriching *CvBV_12-6* in hemocytes may have modulated the host immune response. As an effective system to

study proteins of unknown function, the *D. melanogaster* model has been employed in the study of the function of BV virulence genes [59], and we used this model in our study. As a nonmodal organism, no effective genetic manipulation has been performed to explore functional proteins in *P. xylostella*, especially exogenous gene products of PDV that integrate into the host genome after embryonic development. In this study, RNAi was chosen as the optimal system for testing the effect of virulence factors. Although gene knockdown is difficult to achieve in Lepidoptera, the effectiveness of PDV gene interference is relatively high, with a 70–80%, and sometimes a 90%, decrease in target gene expression [60,61]. In addition, it is a technical challenge to overexpress genes in Lepidoptera, and previous studies have used baculovirus as a transient expression system to analyze CvBV-gene cellular immune responses [40,62,63]. Therefore, we took advantage of the Bac-to-Bac baculovirus expression system, which enables the rapid and efficient expression of target genes. NPV was injected into the *P. xylostella* larvae and infected the tissues, leading to the expression of the CvBV_12-6 protein. To exclude the effect of baculovirus infection on *P. xylostella*, we strictly examined the response of hemocytes within 24 h, in which CvBV_12-6 was highly expressed, and there were no obvious symptoms caused by baculovirus infection. Additionally, the negative control NPV-GFP was an important reference for the interpretation of the results. Taken together, the results of this study show evidence for the potential function of bracovirus PTPs.

There are some commonalities and differences among the function of CvBV_12-6 in *D. melanogaster* and *P. xylostella*. The difference is that CvBV_12-6 did not change the viability of hemocytes in *D. melanogaster*, but impaired that in the host *P. xylostella*, which may have been a result of the genetic difference between these two species. Concerning a decrease in host hemocyte viability, some BV PTPs have been shown to induce apoptosis in the Sf21 cell line via caspase activation [39]. However, this does not seem to be the cause for CvBV_12-6 because the total number of host hemocytes was not affected. Cell death and survival involve multiple processes; therefore, more experiments are needed to explore the role of CvBV_12-6 in inducing host cell death. CvBV_12-6 inhibited melanization reactions in both insects, consistent with early findings after *C. vestalis* parasitization [55,64] and CvBV injection [55]. Although the mechanism via which CvBV_12-6 regulates host melanization remains unclear, the regulation of phosphorylation levels during melanization in *D. melanogaster* has been extensively studied. In *D. melanogaster*, p38 MAPKs are preferentially activated in response to a wide variety of stress stimuli, and thereafter phosphorylate various substrates to regulate cellular immune and stress responses [65–67]. Sekine et al. found that p38 functions in the dopamine synthesis pathway to activate the melanization reaction and may be involved in immune and stress responses [68]. Therefore, we propose that CvBV_12-6 may inhibit melanization by negatively regulating the MAPK pathway or directly suppressing the survival of hemocytes in the *P. xylostella* host. Furthermore, our previous studies have shown that CLP genes in CvBV [55] and a trypsin inhibitor-like protein [69] in teratocytes functioned as melanization inhibitors, indicating multistep regulation of the host PO pathway mediated by parasitic wasp-associated factors.

In summary, we identified a PTP gene in *C. vestalis* BV, CvBV_12-6, that showed tyrosine phosphatase activity. CvBV_12-6 inhibited both the cellular and humoral immunity of *P. xylostella* by reducing the hemocyte viability or suppressing phenoloxidase/melanization responses individually, and it also showed functional immunosuppression in the ectopic host *D. melanogaster*. Our results not only provide evidence for an inhibitory role played by a newly characterized gene family (PTP) in the host melanization response, but also expand our knowledge about the mechanisms by which parasitoids regulate the humoral immunity of their hosts.

Author Contributions: Conceptualization, supervision, and funding acquisition, X.-X.C. and Z.-Z.W.; software, Z.-H.W.; validation, H.-S.G., X.-Q.Y. and R.-M.H.; formal analysis, X.-T.W.; investigation, R.-M.H. and H.-S.G.; resources, R.-M.H. and H.-S.G.; writing—original draft preparation H.-S.G.; writing—review and editing, Z.-Z.W., J.-H.H. and X.-X.C. All authors have read and agreed to the published version of the manuscript.

Funding: This research was funded by the Guangdong Laboratory of Lingnan Modern Agriculture Project (NT2021003), the National Key Research and Development Plan (2019YFD1002101), and the Key R&D Program of Zhejiang Province (2021C02045).

Institutional Review Board Statement: Not applicable.

Informed Consent Statement: Not applicable.

Data Availability Statement: Not applicable.

Acknowledgments: We thank Si-Cong Zhou and Shi-Min Zhou for their technical support during the course of this study.

Conflicts of Interest: The authors declare no conflict of interest.

References

1. Strand, M.R.; Burke, G.R. Polydnavirus-wasp associations: Evolution, genome organization, and function. *Curr. Opin. Virol.* **2013**, *3*, 587–594. [[CrossRef](#)] [[PubMed](#)]
2. Volkoff, A.N.; Cusson, M. The unconventional viruses of ichneumonid parasitoid wasps. *Viruses* **2020**, *12*, 1170. [[CrossRef](#)] [[PubMed](#)]
3. Strand, M.R.; Burke, G.R. Polydnaviruses: Nature’s genetic engineers. *Annu. Rev. Virol.* **2014**, *1*, 333–354. [[CrossRef](#)] [[PubMed](#)]
4. Bézier, A.; Annaheim, M.; Herbinière, J.; Wetterwald, C.; Gyapay, G.; Bernard-Samain, S.; Wincker, P.; Roditi, I.; Heller, M.; Belghazi, M.; et al. Polydnaviruses of braconid wasps derive from an ancestral nudivirus. *Science* **2009**, *323*, 926–930. [[CrossRef](#)] [[PubMed](#)]
5. Strand, M.R.; Burke, G.R. Polydnaviruses: From discovery to current insights. *Virology* **2015**, *479–480*, 393–402. [[CrossRef](#)] [[PubMed](#)]
6. Ye, X.Q.; Shi, M.; Huang, J.H.; Chen, X.X. Parasitoid polydnaviruses and immune interaction with secondary hosts. *Dev. Comp. Immunol.* **2018**, *83*, 124–129. [[CrossRef](#)]
7. Zhang, P.; Turnbull, M. Polydnavirus Innexins disrupt host cellular encapsulation and larval maturation. *Viruses* **2021**, *13*, 1621. [[CrossRef](#)]
8. Shelby, K.S.; Webb, B.A. Polydnavirus-mediated suppression of insect immunity. *J. Insect Physiol.* **1999**, *45*, 507–514. [[CrossRef](#)]
9. Glatz, R.V.; Asgari, S.; Schmidt, O. Evolution of polydnaviruses as insect immune suppressors. *Trends Microbiol.* **2004**, *12*, 545–554. [[CrossRef](#)]
10. Lavine, M.H.; Strand, M.R. A novel polydnavirus protein inhibits the insect prophenoloxidase activation pathway. *Proc. Natl. Acad. Sci. USA* **2007**, *104*, 19267–19272.
11. Lu, Z.; Beck, M.H.; Strand, M.R. Egf1.5 is a second phenoloxidase cascade inhibitor encoded by *Microplitis demolitor* bracovirus. *Insect Biochem. Mol. Biol.* **2010**, *40*, 497–505. [[CrossRef](#)] [[PubMed](#)]
12. Bitra, K.; Suderman, R.J.; Strand, M.R. Polydnavirus Ank proteins bind NF- κ B homodimers and inhibit processing of Relish. *PLoS Pathog* **2012**, *8*, e1002722. [[CrossRef](#)] [[PubMed](#)]
13. Thoetkiattikul, H.; Beck, M.H.; Strand, M.R. Inhibitor kappaB-like proteins from a polydnavirus inhibit NF-kappaB activation and suppress the insect immune response. *Proc. Natl. Acad. Sci. USA* **2005**, *102*, 11426–11431. [[CrossRef](#)] [[PubMed](#)]
14. Zhou, G.F.; Chen, C.X.; Cai, Q.C.; Yan, X.; Peng, N.N.; Li, X.C.; Cui, J.H.; Han, Y.F.; Zhang, Q.; Meng, J.H.; et al. Bracovirus sneaks into apoptotic bodies transmitting immunosuppressive signalling driven by integration-mediated eIF5A hypusination. *Front. Immunol.* **2022**, *13*, 901593. [[CrossRef](#)] [[PubMed](#)]
15. Chen, C.X.; He, H.J.; Cai, Q.C.; Zhang, W.; Kou, T.C.; Zhang, X.W.; You, S.; Chen, Y.B.; Liu, T.; Xiao, W.; et al. Bracovirus-mediated innexin hemichannel closure in cell disassembly. *iScience* **2021**, *24*, 102281. [[CrossRef](#)]
16. Van Eekelen, M.; Runtuwene, V.; Overvoorde, J.; den Hertog, J. RPTP alpha and PTP epsilon signaling via Fyn/Yes and RhoA is essential for zebrafish convergence and extension cell movements during gastrulation. *Dev. Biol.* **2010**, *340*, 626–639. [[CrossRef](#)]
17. Chan, R.J.; Johnson, S.A.; Li, Y.J.; Yoder, M.C.; Feng, G.S. A definitive role of Shp-2 tyrosine phosphatase in mediating embryonic stem cell differentiation and hematopoiesis. *Blood* **2003**, *102*, 2074–2080. [[CrossRef](#)]
18. He, Z.; Zhu, H.H.; Bauler, T.J.; Wang, J.; Ciaraldi, T.; Alderson, N.; Li, S.W.; Raquil, M.A.; Ji, K.H.; Wang, S.F.; et al. Nonreceptor tyrosine phosphatase Shp2 promotes adipogenesis through inhibition of p38 MAP kinase. *Proc. Natl. Acad. Sci. USA* **2013**, *110*, E79–E88. [[CrossRef](#)]
19. Tao, J.; Zheng, L.; Meng, M.; Li, Y.; Lu, Z. Shp2 suppresses the adipogenic differentiation of preadipocyte 3T3-L1 cells at an early stage. *Cell Death Discov.* **2016**, *2*, 16051. [[CrossRef](#)]
20. Matulka, K.; Lin, H.H.; Hribkova, H.; Uwanogho, D.; Dvorak, P.; Sun, Y.M. PTP1B is an effector of activin signaling and regulates neural specification of embryonic stem cells. *Cell Stem Cell* **2013**, *13*, 706–719. [[CrossRef](#)]
21. Mustelin, T.; Vang, T.; Bottini, N. Protein tyrosine phosphatases and the immune response. *Nat. Rev. Immunol.* **2005**, *5*, 43–57. [[CrossRef](#)] [[PubMed](#)]
22. Tailor, P.; Gilman, J.; Williams, S.; Couture, C.; Mustelin, T. Regulation of the low molecular weight phosphotyrosine phosphatase by phosphorylation at tyrosines 131 and 132. *J. Biol. Chem.* **1997**, *272*, 5371–5374. [[CrossRef](#)] [[PubMed](#)]

23. Alonso, A.; Saxena, M.; Williams, S.; Mustelin, T. Inhibitory role for dual specificity phosphatase VHR in T cell antigen receptor and CD28-induced Erk and Jnk activation. *J. Biol. Chem.* **2001**, *276*, 4766–4771. [[CrossRef](#)] [[PubMed](#)]
24. Elchebly, M.; Payette, P.; Michaliszyn, E.; Cromlish, W.; Collins, S.; Loy, A.L.; Normandin, D.; Cheng, A.; Himms-Hagen, J.; Chan, C.C.; et al. Increased insulin sensitivity and obesity resistance in mice lacking the protein tyrosine phosphatase-1B gene. *Science* **1999**, *283*, 1544–1548. [[CrossRef](#)]
25. Neel, B.G.; Tonks, N.K. Protein tyrosine phosphatases in signal transduction. *Curr. Opin. Cell Biol.* **1997**, *9*, 193–204. [[CrossRef](#)] [[PubMed](#)]
26. Chen, Y.P.; Taylor, P.B.; Shapiro, M.; Gundersen-Rindal, D.E. Quantitative expression analysis of a *Glyptapanteles indiensis* polydnavirus protein tyrosine phosphatase gene in its natural lepidopteran host, *Lymantria dispar*. *Insect Mol. Biol.* **2003**, *12*, 271–280. [[CrossRef](#)]
27. Webb, B.A.; Strand, M.R.; Dickey, S.E.; Beck, M.H.; Hilgarth, R.S.; Barney, W.E.; Kadash, K.; Kroemer, J.A.; Lindstrom, K.G.; Rattanadechakul, W.; et al. Polydnavirus genomes reflect their dual roles as mutualists and pathogens. *Virology* **2006**, *347*, 160–174. [[CrossRef](#)]
28. Desjardins, C.A.; Gundersen-Rindal, D.E.; Hostetler, J.B.; Tallon, L.J.; Fadrosh, D.W.; Fuester, R.W.; Pedroni, M.J.; Haas, B.J.; Schatz, M.C.; Jones, K.M.; et al. Comparative genomics of mutualistic viruses of *Glyptapanteles* parasitic wasps. *Genome Biol.* **2008**, *9*, R183. [[CrossRef](#)]
29. Chen, Y.F.; Gao, F.; Ye, X.Q.; Wei, S.J.; Shi, M.; Zheng, H.J.; Chen, X.X. Deep sequencing of *Cotesia vestalis* bracovirus reveals the complexity of a polydnavirus genome. *Virology* **2011**, *414*, 42–50. [[CrossRef](#)]
30. Bézier, A.; Louis, F.; Jancek, S.; Periquet, G.; Thézé, J.; Gyapay, G.; Musset, K.; Lesobre, J.; Lenoble, P.; Dupuy, C.; et al. Functional endogenous viral elements in the genome of the parasitoid wasp *Cotesia congregata*: Insights into the evolutionary dynamics of bracoviruses. *Philos. Trans. R. Soc. B Biol. Sci.* **2013**, *368*, 20130047. [[CrossRef](#)]
31. Jancek, S.; Bézier, A.; Gayral, P.; Paillusson, C.; Kaiser, L.; Dupas, S.; Le Ru, B.P.; Barbe, V.; Periquet, G.; Drezen, J.M.; et al. Adaptive selection on bracovirus genomes drives the specialization of *Cotesia* parasitoid wasps. *PLoS ONE* **2013**, *8*, e64432. [[CrossRef](#)] [[PubMed](#)]
32. Yu, D.S.; Chen, Y.B.; Li, M.; Yang, M.J.; Yang, Y.; Hu, J.S.; Luo, K.J. A polydnal viral genome of *Microplitis bicoloratus* bracovirus and molecular interactions between the host and virus involved in NF- κ B signaling. *Arch. Virol.* **2016**, *161*, 3095–3124. [[CrossRef](#)] [[PubMed](#)]
33. Shi, M.; Chen, Y.F.; Yao, Y.; Huang, F.; Chen, X.X. Characterization of a protein tyrosine phosphatase gene CvBV202 from *Cotesia vestalis* polydnavirus (CvBV). *Virus Genes* **2008**, *36*, 595–601. [[CrossRef](#)] [[PubMed](#)]
34. Mao, M.; Strand, M.R.; Burke, G.R. The complete genome of *Chelonius insularis* reveals dynamic arrangement of genome components in parasitoid wasps That produce bracoviruses. *J Virol* **2022**, *96*, e0157321. [[CrossRef](#)]
35. Serbielle, C.; Dupas, S.; Perdereau, E.; Héricourt, F.; Dupuy, C.; Huguet, E.; Drezen, J.M. Evolutionary mechanisms driving the evolution of a large polydnavirus gene family coding for protein tyrosine phosphatases. *BMC Evol. Biol.* **2012**, *12*, 253. [[CrossRef](#)]
36. Andersen, J.N.; Mortensen, O.H.; Peters, G.H.; Drake, P.G.; Iversen, L.F.; Olsen, O.H.; Jansen, P.G.; Andersen, H.S.; Tonks, N.K.; Moller, N.P.H. Structural and evolutionary relationships among protein tyrosine phosphatase domains. *Mol. Cell. Biol.* **2001**, *21*, 7117–7136. [[CrossRef](#)]
37. Provost, B.; Varricchio, P.; Arana, E.; Espagne, E.; Falabella, P.; Huguet, E.; La Scaleia, R.; Cattolico, L.; Poirié, M.; Malva, C.; et al. Bracoviruses contain a large multigene family coding for protein tyrosine phosphatases. *J Virol* **2004**, *78*, 13090–13103. [[CrossRef](#)]
38. Pruijssers, A.J.; Strand, M.R. PTP-H2 and PTP-H3 from *Microplitis demolitor* bracovirus localize to focal adhesions and are antiphagocytic in insect immune cells. *J. Virol.* **2007**, *81*, 1209–1219. [[CrossRef](#)]
39. Suderman, R.J.; Pruijssers, A.J.; Strand, M.R. Protein tyrosine phosphatase-H2 from a polydnavirus induces apoptosis of insect cells. *J. Gen. Virol.* **2008**, *89 Pt 6*, 1411–1420. [[CrossRef](#)]
40. Ibrahim, A.M.; Kim, Y. Transient expression of protein tyrosine phosphatases encoded in *Cotesia plutellae* bracovirus inhibits insect cellular immune responses. *Naturwissenschaften* **2008**, *95*, 25–32. [[CrossRef](#)]
41. Falabella, P.; Caccialupi, P.; Varricchio, P.; Malva, C.; Pennacchio, F. Protein tyrosine phosphatases of *Toxoneuron nigriceps* bracovirus as potential disrupters of host prothoracic gland function. *Arch Insect Biochem Physiol* **2006**, *61*, 157–169. [[CrossRef](#)] [[PubMed](#)]
42. Salvia, R.; Nardiello, M.; Scieuzo, C.; Scala, A.; Bufo, S.A.; Rao, A.; Vogel, H.; Falabella, P. Novel factors of viral origin inhibit TOR pathway gene expression. *Front. Physiol.* **2018**, *9*, 1678. [[CrossRef](#)] [[PubMed](#)]
43. Zalucki, M.P.; Shabbir, A.; Silva, R.; Adamson, D.; Shu-Sheng, L.; Furlong, M.J. Estimating the economic cost of one of the world's major insect pests, *Plutella xylostella* (Lepidoptera: Plutellidae): Just how long is a piece of string? *J. Econ. Entomol.* **2012**, *105*, 1115–1129. [[CrossRef](#)] [[PubMed](#)]
44. Wang, Z.H.; Ye, X.Q.; Zhou, Y.N.; Wu, X.T.; Hu, R.M.; Zhu, J.C.; Chen, T.; Huguet, E.; Shi, M.; Drezen, J.M.; et al. Bracoviruses recruit host integrases for their integration into caterpillar's genome. *PLoS Genet* **2021**, *17*, e1009751. [[CrossRef](#)] [[PubMed](#)]
45. Chen, Y.F.; Shi, M.; Liu, P.C.; Huang, F.; Chen, X.X. Characterization of an IkappaB-like gene in *Cotesia vestalis* polydnavirus. *Arch. Insect Biochem. Physiol.* **2008**, *68*, 71–78. [[CrossRef](#)]
46. Livak, K.J.; Schmittgen, T.D. Analysis of relative gene expression data using real-time quantitative PCR and the 2(-Delta Delta C(T)) Method. *Methods* **2001**, *25*, 402–408. [[CrossRef](#)]

47. Philipps, B.; Rotmann, D.; Wicki, M.; Mayr, L.M.; Forstner, M. Time reduction and process optimization of the baculovirus expression system for more efficient recombinant protein production in insect cells. *Protein Expr. Purif.* **2005**, *42*, 211–218. [[CrossRef](#)]
48. Brand, A.H.; Perrimon, N. Targeted gene expression as a means of altering cell fates and generating dominant phenotypes. *Development* **1993**, *118*, 401–415. [[CrossRef](#)]
49. Bischof, J.; Maeda, R.K.; Hediger, M.; Karch, F.; Basler, K. An optimized transgenesis system for *Drosophila* using germ-line-specific phiC31 integrases. *Proc. Natl. Acad. Sci. USA* **2007**, *104*, 3312–3317. [[CrossRef](#)]
50. Sinenko, S.A.; Kim, E.K.; Wynn, R.; Manfrulli, P.; Ando, I.; Wharton, K.A.; Perrimon, N.; Mathey-Prevot, B. Yantar, a conserved arginine-rich protein is involved in *Drosophila* hemocyte development. *Dev. Biol.* **2004**, *273*, 48–62. [[CrossRef](#)]
51. Wang, Z.H.; Hu, R.M.; Ye, X.Q.; Huang, J.H.; Chen, X.X.; Shi, M. Laccase 1 gene from *Plutella xylostella* (PxLac1) and its functions in humoral immune response. *J. Insect Physiol.* **2018**, *107*, 197–203. [[CrossRef](#)] [[PubMed](#)]
52. Goldsworthy, G.; Chandrakant, S.; Opoku-Ware, K. Adipokinetic hormone enhances nodule formation and phenoloxidase activation in adult locusts injected with bacterial lipopolysaccharide. *J. Insect Physiol.* **2003**, *49*, 795–803. [[CrossRef](#)] [[PubMed](#)]
53. Qi, Y.X.; Huang, J.; Li, M.Q.; Wu, Y.S.; Xia, R.Y.; Ye, G.Y. Serotonin modulates insect hemocyte phagocytosis via two different serotonin receptors. *eLife* **2016**, *5*, e12241. [[CrossRef](#)] [[PubMed](#)]
54. Cheung, G.Y.C.; Bae, J.S.; Otto, M. Pathogenicity and virulence of *Staphylococcus aureus*. *Virulence* **2021**, *12*, 547–569. [[CrossRef](#)] [[PubMed](#)]
55. Wang, Z.H.; Zhou, Y.N.; Ye, X.Q.; Wu, X.T.; Yang, P.; Shi, M.; Huang, J.H.; Chen, X.X. CLP gene family, a new gene family of *Cotesia vestalis* bracovirus inhibits melanization of *Plutella xylostella* hemolymph. *Insect Sci.* **2021**, *28*, 1567–1581. [[CrossRef](#)]
56. Flint, A.J.; Tiganis, T.; Barford, D.; Tonks, N.K. Development of “substrate-trapping” mutants to identify physiological substrates of protein tyrosine phosphatases. *Proc. Natl. Acad. Sci. USA* **1997**, *94*, 1680–1685. [[CrossRef](#)]
57. Van Vactor, D.; O’Reilly, A.M.; Neel, B.G. Genetic analysis of protein tyrosine phosphatases. *Curr. Opin. Genet. Dev.* **1998**, *8*, 112–126. [[CrossRef](#)]
58. Lavine, M.D.; Strand, M.R. Insect hemocytes and their role in immunity. *Insect Biochem. Mol. Biol.* **2002**, *32*, 1295–1309. [[CrossRef](#)]
59. Ignesti, M.; Ferrara, R.; Romani, P.; Valzania, L.; Serafini, G.; Pennacchio, F.; Cavaliere, V.; Gargiulo, G. A polydnavirus-encoded ANK protein has a negative impact on steroidogenesis and development. *Insect Biochem. Mol. Biol.* **2018**, *95*, 26–32. [[CrossRef](#)]
60. Wu, X.; Wu, Z.; Ye, X.; Pang, L.; Sheng, Y.; Wang, Z.; Zhou, Y.; Zhu, J.; Hu, R.; Zhou, S.; et al. The dual functions of a Bracovirus C-Type Lectin in Caterpillar immune response manipulation. *Front. Immunol.* **2022**, *13*, 877027. [[CrossRef](#)] [[PubMed](#)]
61. Di Lelio, I.; Illiano, A.; Astarita, F.; Gianfranceschi, L.; Horner, D.; Varricchio, P.; Amoresano, A.; Pucci, P.; Pennacchio, F.; Caccia, S. Evolution of an insect immune barrier through horizontal gene transfer mediated by a parasitic wasp. *PLoS Genet.* **2019**, *15*, e1007998. [[CrossRef](#)] [[PubMed](#)]
62. Kwon, B.; Kim, Y. Transient expression of an EP1-like gene encoded in *Cotesia plutellae* bracovirus suppresses the hemocyte population in the diamondback moth, *Plutella xylostella*. *Dev. Comp. Immunol.* **2008**, *32*, 932–942. [[CrossRef](#)] [[PubMed](#)]
63. Gad, W.; Kim, Y. A viral histone H4 encoded by *Cotesia plutellae* bracovirus inhibits haemocyte-spreading behaviour of the diamondback moth, *Plutella xylostella*. *J. Gen. Virol.* **2008**, *89 Pt 4*, 931–938. [[CrossRef](#)] [[PubMed](#)]
64. Bae, S.; Kim, Y. Host physiological changes due to parasitism of a braconid wasp, *Cotesia plutellae*, on diamondback moth, *Plutella xylostella*. *Comp. Biochem. Physiol. A Mol. Integr. Physiol.* **2004**, *138*, 39–44. [[CrossRef](#)] [[PubMed](#)]
65. Widmann, C.; Gibson, S.; Jarpe, M.B.; Johnson, G.L. Mitogen-activated protein kinase: Conservation of a three-kinase module from yeast to human. *Physiol. Rev.* **1999**, *79*, 143–180. [[CrossRef](#)] [[PubMed](#)]
66. Kyriakis, J.M.; Avruch, J. Mammalian mitogen-activated protein kinase signal transduction pathways activated by stress and inflammation. *Physiol. Rev.* **2001**, *81*, 807–869. [[CrossRef](#)] [[PubMed](#)]
67. Zarubin, T.; Han, J. Activation and signaling of the p38 MAP kinase pathway. *Cell Res.* **2005**, *15*, 11–18. [[CrossRef](#)]
68. Sekine, Y.; Takagahara, S.; Hatanaka, R.; Watanabe, T.; Oguchi, H.; Noguchi, T.; Naguro, I.; Kobayashi, K.; Tsunoda, M.; Funatsu, T.; et al. p38 MAPKs regulate the expression of genes in the dopamine synthesis pathway through phosphorylation of NR4A nuclear receptors. *J. Cell Sci.* **2011**, *124 Pt 17*, 3006–3016. [[CrossRef](#)]
69. Gu, Q.J.; Zhou, S.M.; Zhou, Y.N.; Huang, J.H.; Shi, M.; Chen, X.X. A trypsin inhibitor-like protein secreted by *Cotesia vestalis* teratocytes inhibits hemolymph prophenoloxidase activation of *Plutella xylostella*. *J. Insect Physiol.* **2019**, *116*, 41–48. [[CrossRef](#)]

Disclaimer/Publisher’s Note: The statements, opinions and data contained in all publications are solely those of the individual author(s) and contributor(s) and not of MDPI and/or the editor(s). MDPI and/or the editor(s) disclaim responsibility for any injury to people or property resulting from any ideas, methods, instructions or products referred to in the content.